CHAPTER 4

Inverse manipulator kinematics

4.1 INTRODUCTION
4.2 SOLVABILITY
4.3 THE NOTION OF MANIPULATOR SUBSPACE WHEN $n < 6$
4.4 ALGEBRAIC VS. GEOMETRIC
4.5 ALGEBRAIC SOLUTION BY REDUCTION TO POLYNOMIAL
4.6 PIEPER'S SOLUTION WHEN THREE AXES INTERSECT
4.7 EXAMPLES OF INVERSE MANIPULATOR KINEMATICS
4.8 THE STANDARD FRAMES
4.9 SOLVE-ING A MANIPULATOR
4.10 REPEATABILITY AND ACCURACY
4.11 COMPUTATIONAL CONSIDERATIONS

4.1 INTRODUCTION

In the last chapter, we considered the problem of computing the position and orientation of the tool relative to the user's workstation when given the joint angles of the manipulator. In this chapter, we investigate the more difficult converse problem: Given the desired position and orientation of the tool relative to the station, how do we compute the set of joint angles which will achieve this desired result? Whereas Chapter 3 focused on the **direct kinematics** of manipulators, here the focus is the **inverse kinematics** of manipulators.

Solving the problem of finding the required joint angles to place the tool frame, $\{T\}$, relative to the station frame, $\{S\}$, is split into two parts. First, frame transformations are performed to find the wrist frame, $\{W\}$, relative to the base frame, $\{B\}$, and then the inverse kinematics are used to solve for the joint angles.

4.2 SOLVABILITY

The problem of solving the kinematic equations of a manipulator is a nonlinear one. Given the numerical value of ${}^0_N T$, we attempt to find values of $\theta_1, \theta_2, \ldots, \theta_n$. Consider the equations given in (3.14). In the case of the PUMA 560 manipulator, the precise statement of our current problem is as follows: Given ${}^0_6 T$ as sixteen numeric values (four of which are trivial), solve (3.14) for the six joint angles θ_1 through θ_6.

For the case of an arm with six degrees of freedom (like the one corresponding to the equations in (3.14)), we have 12 equations and six unknowns. However, among the 9 equations arising from the rotation-matrix portion of ${}^0_6 T$, only 3 are independent. These, added to the 3 equations from the position-vector portion of ${}^0_6 T$,

give 6 equations with six unknowns. These equations are nonlinear, transcendental equations, which can be quite difficult to solve. The equations of (3.14) are those of a robot that had very simple link parameters—many of the α_i were 0 or ± 90 degrees. Many link offsets and lengths were zero. It is easy to imagine that, for the case of a general mechanism with six degrees of freedom (with all link parameters nonzero) the kinematic equations would be much more complex than those of (3.14). As with any nonlinear set of equations, we must concern ourselves with the existence of solutions, with multiple solutions, and with the method of solution.

Existence of solutions

The question of whether any solution exists at all raises the question of the manipulator's **workspace**. Roughly speaking, workspace is that volume of space that the end-effector of the manipulator can reach. For a solution to exist, the specified goal point must lie within the workspace. Sometimes, it is useful to consider two definitions of workspace: **Dextrous workspace** is that volume of space that the robot end-effector can reach with all orientations. That is, at each point in the dextrous workspace, the end-effector can be arbitrarily oriented. The **reachable workspace** is that volume of space that the robot can reach in at least one orientation. Clearly, the dextrous workspace is a subset of the reachable workspace.

Consider the workspace of the two-link manipulator in Fig. 4.1. If $l_1 = l_2$, then the reachable workspace consists of a disc of radius $2l_1$. The dextrous workspace consists of only a single point, the origin. If $l_1 \neq l_2$, then there is no dextrous workspace, and the reachable workspace becomes a ring of outer radius $l_1 + l_2$ and inner radius $|l_1 - l_2|$. Inside the reachable workspace there are two possible orientations of the end-effector. On the boundaries of the workspace there is only one possible orientation.

These considerations of workspace for the two-link manipulator have assumed that all the joints can rotate 360 degrees. This is rarely true for actual mechanisms. When joint limits are a subset of the full 360 degrees, then the workspace is obviously correspondingly reduced, either in extent, or in the number of possible orientations

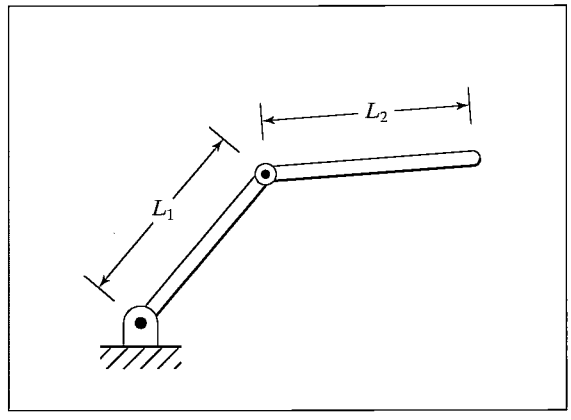

FIGURE 4.1: Two-link manipulator with link lengths l_1 and l_2.

attainable. For example, if the arm in Fig. 4.1 has full 360-degree motion for θ_1, but only $0 \leq \theta_2 \leq 180°$, then the reachable workspace has the same extent, but only one orientation is attainable at each point.

When a manipulator has fewer than six degrees of freedom, it cannot attain general goal positions and orientations in 3-space. Clearly, the planar manipulator in Fig. 4.1 cannot reach out of the plane, so any goal point with a nonzero Z-coordinate value can be quickly rejected as unreachable. In many realistic situations, manipulators with four or five degrees of freedom are employed that operate out of a plane, but that clearly cannot reach general goals. Each such manipulator must be studied to understand its workspace. In general, the workspace of such a robot is a subset of a subspace that can be associated with any particular robot. Given a general goal-frame specification, an interesting problem arises in connection with manipulators having fewer than six degrees of freedom: What is the nearest attainable goal frame?

Workspace also depends on the tool-frame transformation, because it is usually the tool-tip that is discussed when we speak of reachable points in space. Generally, the tool transformation is performed independently of the manipulator kinematics and inverse kinematics, so we are often led to consider the workspace of the wrist frame, $\{W\}$. For a given end-effector, a tool frame, $\{T\}$, is defined; given a goal frame, $\{G\}$, the corresponding $\{W\}$ frame is calculated, and then we ask: Does this desired position and orientation of $\{W\}$ lie in the workspace? In this way, the workspace that we must concern ourselves with (in a computational sense) is different from the one imagined by the user, who is concerned with the workspace of the end-effector (the $\{T\}$ frame).

If the desired position and orientation of the wrist frame is in the workspace, then at least one solution exists.

Multiple solutions

Another possible problem encountered in solving kinematic equations is that of multiple solutions. A planar arm with three revolute joints has a large dextrous workspace in the plane (given "good" link lengths and large joint ranges), because any position in the interior of its workspace can be reached with any orientation. Figure 4.2 shows a three-link planar arm with its end-effector at a certain position

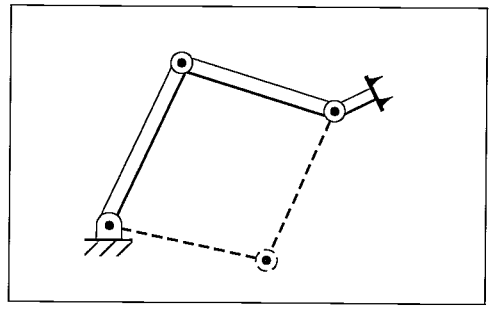

FIGURE 4.2: Three-link manipulator. Dashed lines indicate a second solution.

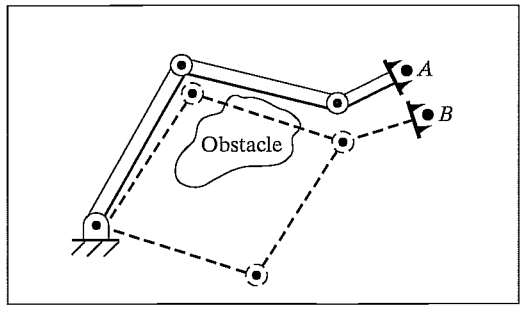

FIGURE 4.3: One of the two possible solutions to reach point B causes a collision.

and orientation. The dashed lines indicate a second possible configuration in which the same end-effector position and orientation are achieved.

The fact that a manipulator has multiple solutions can cause problems, because the system has to be able to choose one. The criteria upon which to base a decision vary, but a very reasonable choice would be the *closest* solution. For example, if the manipulator is at point A, as in Fig. 4.3, and we wish to move it to point B, a good choice would be the solution that minimizes the amount that each joint is required to move. Hence, in the absence of the obstacle, the upper dashed configuration in Fig. 4.3 would be chosen. This suggests that one input argument to our kinematic inverse procedure might be the present position of the manipulator. In this way, if there is a choice, our algorithm can choose the solution closest in joint-space. However, the notion of "close" might be defined in several ways. For example, typical robots could have three large links followed by three smaller, orienting links near the end-effector. In this case, weights might be applied in the calculation of which solution is "closer" so that the selection favors moving smaller joints rather than moving the large joints, when a choice exists. The presence of obstacles might force a "farther" solution to be chosen in cases where the "closer" solution would cause a collision—in general, then, we need to be able to calculate all the possible solutions. Thus, in Fig. 4.3, the presence of the obstacle implies that the lower dashed configuration is to be used to reach point B.

The number of solutions depends upon the number of joints in the manipulator but is also a function of the link parameters (α_i, a_i, and d_i for a rotary joint manipulator) and the allowable ranges of motion of the joints. For example, the PUMA 560 can reach certain goals with eight different solutions. Figure 4.4 shows four solutions; all place the hand with the same position and orientation. For each solution pictured, there is another solution in which the last three joints "flip" to an alternate configuration according to the following formulas:

$$\begin{aligned} \theta_4' &= \theta_4 + 180°, \\ \theta_5' &= -\theta_5, \\ \theta_6' &= \theta_6 + 180°. \end{aligned} \tag{4.1}$$

So, in total, there can be eight solutions for a single goal. Because of limits on joint ranges, some of these eight could be inaccessible.

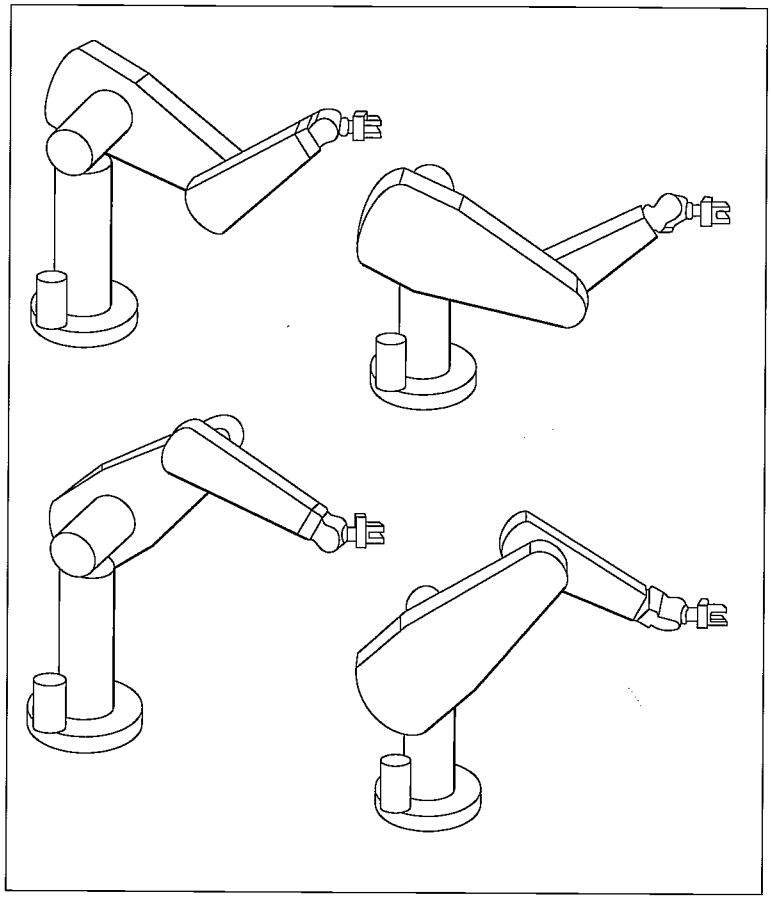

FIGURE 4.4: Four solutions of the PUMA 560.

In general, the more nonzero link parameters there are, the more ways there will be to reach a certain goal. For example, consider a manipulator with six rotational joints. Figure 4.5 shows how the maximum number of solutions is related to how many of the link length parameters (the a_i) are zero. The more that are nonzero, the bigger is the maximum number of solutions. For a completely general rotary-jointed manipulator with six degrees of freedom, there are up to sixteen solutions possible [1, 6].

Method of solution

Unlike linear equations, there are no general algorithms that may be employed to solve a set of nonlinear equations. In considering methods of solution, it will be wise to define what constitutes the "solution" of a given manipulator.

A manipulator will be considered solvable if the joint variables can be determined by an algorithm that allows one to determine *all* the sets of joint variables associated with a given position and orientation [2].

a_i	Number of solutions
$a_1 = a_3 = a_5 = 0$	≤ 4
$a_3 = a_5 = 0$	≤ 8
$a_3 = 0$	≤ 16
All $a_i \neq 0$	≤ 16

FIGURE 4.5: Number of solutions vs. nonzero a_i.

The main point of this definition is that we require, in the case of multiple solutions, that it be possible to calculate all solutions. Hence, we do not consider some numerical iterative procedures as solving the manipulator—namely, those methods not guaranteed to find all the solutions.

We will split all proposed manipulator solution strategies into two broad classes: **closed-form solutions** and **numerical solutions**. Because of their iterative nature, numerical solutions generally are much slower than the corresponding closed-form solution; so much so, in fact, that, for most uses, we are not interested in the numerical approach to solution of kinematics. Iterative numerical solution to kinematic equations is a whole field of study in itself (see [6,11,12]) and is beyond the scope of this text.

We will restrict our attention to closed-form solution methods. In this context, "closed form" means a solution method based on analytic expressions or on the solution of a polynomial of degree 4 or less, such that noniterative calculations suffice to arrive at a solution. Within the class of closed-form solutions, we distinguish two methods of obtaining the solution: **algebraic** and **geometric**. These distinctions are somewhat hazy: Any geometric methods brought to bear are applied by means of algebraic expressions, so the two methods are similar. The methods differ perhaps in approach only.

A major recent result in kinematics is that, according to our definition of solvability, *all systems with revolute and prismatic joints having a total of six degrees of freedom in a single series chain are solvable.* However, this general solution is a numerical one. Only in special cases can robots with six degrees of freedom be solved analytically. These robots for which an analytic (or closed-form) solution exists are characterized either by having several intersecting joint axes or by having many α_i equal to 0 or ± 90 degrees. Calculating numerical solutions is generally time consuming relative to evaluating analytic expressions; hence, it is considered very important to design a manipulator so that a closed-form solution exists. Manipulator designers discovered this very soon, and now virtually all industrial manipulators are designed sufficiently simply that a closed-form solution can be developed.

A sufficient condition that a manipulator with six revolute joints have a closed-form solution is that three neighboring joint axes intersect at a point. Section 4.6 discusses this condition. Almost every manipulator with six degrees of freedom built today has three axes intersecting. For example, axes 4, 5, and 6 of the PUMA 560 intersect.

4.3 THE NOTION OF MANIPULATOR SUBSPACE WHEN $n < 6$

The set of reachable goal frames for a given manipulator constitutes its reachable workspace. For a manipulator with n degrees of freedom (where $n < 6$), this reachable workspace can be thought of as a portion of an n-degree-of-freedom **subspace**. In the same manner in which the workspace of a six-degree-of-freedom manipulator is a subset of space, the workspace of a simpler manipulator is a subset of its subspace. For example, the subspace of the two-link robot of Fig. 4.1 is a plane, but the workspace is a subset of this plane, namely a circle of radius $l_1 + l_2$ for the case that $l_1 = l_2$.

One way to specify the subspace of an n-degree-of-freedom manipulator is to give an expression for its wrist or tool frame as a function of n variables that locate it. If we consider these n variables to be free, then, as they take on all possible values, the subspace is generated.

EXAMPLE 4.1

Give a description of the subspace of ${}^{B}_{W}T$ for the three-link manipulator from Chapter 3, Fig. 3.6.

The subspace of ${}^{B}_{W}T$ is given by

$$ {}^{B}_{W}T = \begin{bmatrix} c_\phi & -s_\phi & 0.0 & x \\ s_\phi & c_\phi & 0.0 & y \\ 0.0 & 0.0 & 1.0 & 0.0 \\ 0 & 0 & 0 & 1 \end{bmatrix}, \tag{4.2} $$

where x and y give the position of the wrist and ϕ describes the orientation of the terminal link. As x, y, and ϕ are allowed to take on arbitrary values, the subspace is generated. Any wrist frame that does not have the structure of (4.2) lies outside the subspace (and therefore lies outside the workspace) of this manipulator. Link lengths and joint limits restrict the workspace of the manipulator to be a subset of this subspace.

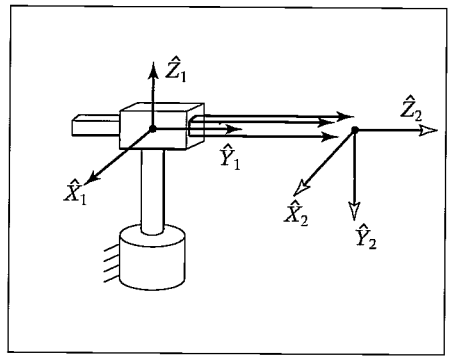

FIGURE 4.6: A polar two-link manipulator.

EXAMPLE 4.2

Give a description of the subspace of ${}^0_2T$ for the polar manipulator with two degrees of freedom shown in Fig. 4.6. We have

$$ {}^0P_{2ORG} = \begin{bmatrix} x \\ y \\ 0 \end{bmatrix}, \tag{4.3} $$

where x and y can take any values. The orientation is restricted because the ${}^0\hat{Z}_2$ axis must point in a direction that depends on x and y. The ${}^0\hat{Y}_2$ axis always points down, and the ${}^0\hat{X}_2$ axis can be computed as the cross product ${}^0\hat{Y}_2 \times {}^0\hat{Z}_2$. In terms of x and y, we have

$$ {}^0\hat{Z}_2 = \begin{bmatrix} \dfrac{x}{\sqrt{x^2+y^2}} \\ \dfrac{y}{\sqrt{x^2+y^2}} \\ 0 \end{bmatrix}. \tag{4.4} $$

The subspace can therefore be given as

$$ {}^0_2T = \begin{bmatrix} \dfrac{y}{\sqrt{x^2+y^2}} & 0 & \dfrac{x}{\sqrt{x^2+y^2}} & x \\ \dfrac{-x}{\sqrt{x^2+y^2}} & 0 & \dfrac{y}{\sqrt{x^2+y^2}} & y \\ 0 & -1 & 0 & 0 \\ 0 & 0 & 0 & 1 \end{bmatrix}. \tag{4.5} $$

Usually, in defining a goal for a manipulator with n degrees of freedom, we use n parameters to specify the goal. If, on the other hand, we give a specification of a full six degrees of freedom, we will not in general be able to reach the goal with an $n < 6$ manipulator. In this case, we might be interested instead in reaching a goal that lies in the manipulator's subspace and is as "near" as possible to the original desired goal.

Hence, when specifying *general* goals for a manipulator with fewer than six degrees of freedom, one solution strategy is the following:

1. Given a general goal frame, ${}^S_GT$, compute a modified goal frame, ${}^S_{G'}T$, such that ${}^S_{G'}T$ lies in the manipulator's subspace and is as "near" to ${}^S_GT$ as possible. A definition of "near" must be chosen.
2. Compute the inverse kinematics to find joint angles using ${}^S_{G'}T$ as the desired goal. Note that a solution still might not be possible if the goal point is not in the manipulator's workspace.

It generally makes sense to position the tool-frame origin to the desired location and then choose an attainable orientation that is near the desired orientation. As we saw in Examples 4.1 and 4.2, computation of the subspace is dependent on manipulator geometry. Each manipulator must be individually considered to arrive at a method of making this computation.

Section 4.7 gives an example of *projecting* a general goal into the subspace of a manipulator with five degrees of freedom in order to compute joint angles that will result in the manipulator's reaching the attainable frame nearest to the desired one.

4.4 ALGEBRAIC VS. GEOMETRIC

As an introduction to solving kinematic equations, we will consider two different approaches to the solution of a simple planar three-link manipulator.

Algebraic solution

Consider the three-link planar manipulator introduced in Chapter 3. It is shown with its link parameters in Fig. 4.7.

Following the method of Chapter 3, we can use the link parameters easily to find the kinematic equations of this arm:

$$ {}^{B}_{W}T = {}^{0}_{3}T = \begin{bmatrix} c_{123} & -s_{123} & 0.0 & l_1c_1 + l_2c_{12} \\ s_{123} & c_{123} & 0.0 & l_1s_1 + l_2s_{12} \\ 0.0 & 0.0 & 1.0 & 0.0 \\ 0 & 0 & 0 & 1 \end{bmatrix}. \tag{4.6} $$

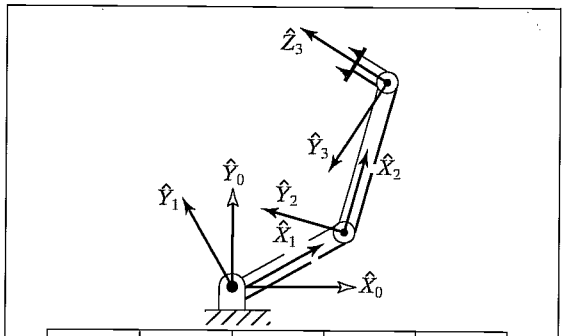

i	$\alpha_i - 1$	$\alpha_i - 1$	d_i	θ_i
1	0	0	0	θ_1
2	0	L_1	0	θ_2
3	0	L_2	0	θ_3

FIGURE 4.7: Three-link planar manipulator and its link parameters.

To focus our discussion on inverse kinematics, we will assume that the necessary transformations have been performed so that the goal point is a specification of the wrist frame relative to the base frame, that is, ${}^{B}_{W}T$. Because we are working with a planar manipulator, specification of these goal points can be accomplished most easily by specifying three numbers: x, y, and ϕ, where ϕ is the orientation of link 3 in the plane (relative to the $+\hat{X}$ axis). Hence, rather than giving a general ${}^{B}_{W}T$ as a goal specification, we will assume a transformation with the structure

$$ {}^{B}_{W}T = \begin{bmatrix} c_\phi & -s_\phi & 0.0 & x \\ s_\phi & c_\phi & 0.0 & y \\ 0.0 & 0.0 & 1.0 & 0.0 \\ 0 & 0 & 0 & 1 \end{bmatrix}. \tag{4.7} $$

All attainable goals must lie in the subspace implied by the structure of equation (4.7). By equating (4.6) and (4.7), we arrive at a set of four nonlinear equations that must be solved for θ_1, θ_2, and θ_3:

$$ c_\phi = c_{123}, \tag{4.8} $$

$$ s_\phi = s_{123}, \tag{4.9} $$

$$ x = l_1 c_1 + l_2 c_{12}, \tag{4.10} $$

$$ y = l_1 s_1 + l_2 s_{12}. \tag{4.11} $$

We now begin our algebraic solution of equations (4.8) through (4.11). If we square both (4.10) and (4.11) and add them, we obtain

$$ x^2 + y^2 = l_1^2 + l_2^2 + 2 l_1 l_2 c_2, \tag{4.12} $$

where we have made use of

$$ \begin{aligned} c_{12} &= c_1 c_2 - s_1 s_2, \\ s_{12} &= c_1 s_2 + s_1 c_2. \end{aligned} \tag{4.13} $$

Solving (4.12) for c_2, we obtain

$$ c_2 = \frac{x^2 + y^2 - l_1^2 - l_2^2}{2 l_1 l_2}. \tag{4.14} $$

In order for a solution to exist, the right-hand side of (4.14) must have a value between -1 and 1. In the solution algorithm, this constraint would be checked at this time to find out whether a solution exists. Physically, if this constraint is not satisfied, then the goal point is too far away for the manipulator to reach.

Assuming the goal is in the workspace, we write an expression for s_2 as

$$ s_2 = \pm\sqrt{1 - c_2^2}. \tag{4.15} $$

Finally, we compute θ_2, using the two-argument arctangent routine[1]:

$$ \theta_2 = \text{Atan2}(s_2, c_2). \tag{4.16} $$

[1] See Section 2.8.

The choice of signs in (4.15) corresponds to the multiple solution in which we can choose the "elbow-up" or the "elbow-down" solution. In determining θ_2, we have used one of the recurring methods for solving the type of kinematic relationships that often arise, namely, to determine both the sine and cosine of the desired joint angle and then apply the two-argument arctangent. This ensures that we have found all solutions and that the solved angle is in the proper quadrant.

Having found θ_2, we can solve (4.10) and (4.11) for θ_1. We write (4.10) and (4.11) in the form

$$x = k_1 c_1 - k_2 s_1, \tag{4.17}$$

$$y = k_1 s_1 + k_2 c_1, \tag{4.18}$$

where

$$\begin{aligned} k_1 &= l_1 + l_2 c_2, \\ k_2 &= l_2 s_2. \end{aligned} \tag{4.19}$$

In order to solve an equation of this form, we perform a change of variables. Actually, we are changing the way in which we write the constants k_1 and k_2.

If

$$r = +\sqrt{k_1^2 + k_2^2} \tag{4.20}$$

and

$$\gamma = \text{Atan2}(k_2, k_1),$$

then

$$\begin{aligned} k_1 &= r\cos\gamma, \\ k_2 &= r\sin\gamma. \end{aligned} \tag{4.21}$$

Equations (4.17) and (4.18) can now be written as

$$\frac{x}{r} = \cos\gamma\cos\theta_1 - \sin\gamma\sin\theta_1, \tag{4.22}$$

$$\frac{y}{r} = \cos\gamma\sin\theta_1 + \sin\gamma\cos\theta_1, \tag{4.23}$$

so

$$\cos(\gamma + \theta_1) = \frac{x}{r}, \tag{4.24}$$

$$\sin(\gamma + \theta_1) = \frac{y}{r}. \tag{4.25}$$

Using the two-argument arctangent, we get

$$\gamma + \theta_1 = \text{Atan2}\left(\frac{y}{r}, \frac{x}{r}\right) = \text{Atan2}(y, x), \tag{4.26}$$

and so

$$\theta_1 = \text{Atan2}(y, x) - \text{Atan2}(k_2, k_1). \tag{4.27}$$

Note that, when a choice of sign is made in the solution of θ_2 above, it will cause a sign change in k_2, thus affecting θ_1. The substitutions used, (4.20) and (4.21), constitute a method of solution of a form appearing frequently in kinematics—namely, that of (4.10) or (4.11). Note also that, if $x = y = 0$, then (4.27) becomes undefined—in this case, θ_1 is arbitrary.

Finally, from (4.8) and (4.9), we can solve for the sum of θ_1 through θ_3:

$$\theta_1 + \theta_2 + \theta_3 = \text{Atan2}(s_\phi, c_\phi) = \phi. \tag{4.28}$$

From this, we can solve for θ_3, because we know the first two angles. It is typical with manipulators that have two or more links moving in a plane that, in the course of solution, expressions for sums of joint angles arise.

In summary, an algebraic approach to solving kinematic equations is basically one of manipulating the given equations into a form for which a solution is known. It turns out that, for many common geometries, several forms of transcendental equations commonly arise. We have encountered a couple of them in this preceding section. In Appendix C, more are listed.

Geometric solution

In a geometric approach to finding a manipulator's solution, we try to decompose the spatial geometry of the arm into several plane-geometry problems. For many manipulators (particularly when the $\alpha_i = 0$ or ± 90) this can be done quite easily. Joint angles can then be solved for by using the tools of plane geometry [7]. For the arm with three degrees of freedom shown in Fig. 4.7, because the arm is planar, we can apply plane geometry directly to find a solution.

Figure 4.8 shows the triangle formed by l_1, l_2, and the line joining the origin of frame {0} with the origin of frame {3}. The dashed lines represent the other possible configuration of the triangle, which would lead to the same position of the frame {3}. Considering the solid triangle, we can apply the "law of cosines" to solve for θ_2:

$$x^2 + y^2 = l_1^2 + l_2^2 - 2l_1 l_2 \cos(180 + \theta_2). \tag{4.29}$$

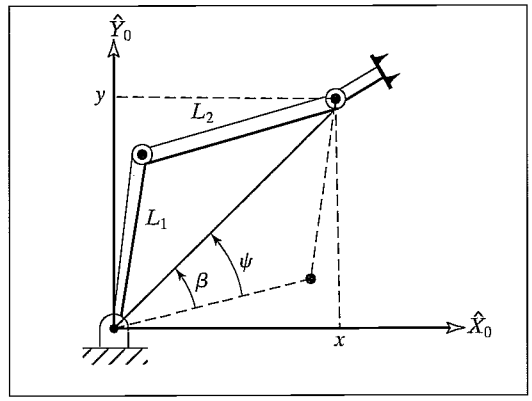

FIGURE 4.8: Plane geometry associated with a three-link planar robot.

Now; $\cos(180 + \theta_2) = -\cos(\theta_2)$, so we have

$$c_2 = \frac{x^2 + y^2 - l_1^2 - l_2^2}{2l_1 l_2}. \tag{4.30}$$

In order for this triangle to exist, the distance to the goal point $\sqrt{x^2 + y^2}$ must be less than or equal to the sum of the link lengths, $l_1 + l_2$. This condition would be checked at this point in a computational algorithm to verify existence of solutions. This condition is not satisfied when the goal point is out of reach of the manipulator. Assuming a solution exists, this equation is solved for that value of θ_2 that lies between 0 and -180 degrees, because only for these values does the triangle in Fig. 4.8 exist. The other possible solution (the one indicated by the dashed-line triangle) is found by symmetry to be $\theta_2' = -\theta_2$.

To solve for θ_1, we find expressions for angles ψ and β as indicated in Fig. 4.8. First, β may be in any quadrant, depending on the signs of x and y. So we must use a two-argument arctangent:

$$\beta = \text{Atan2}(y, x). \tag{4.31}$$

We again apply the law of cosines to find ψ:

$$\cos\psi = \frac{x^2 + y^2 + l_1^2 - l_2^2}{2l_1\sqrt{x^2 + y^2}}. \tag{4.32}$$

Here, the arccosine must be solved so that $0 \leq \psi \leq 180°$, in order that the geometry which leads to (4.32) will be preserved. These considerations are typical when using a geometric approach—we must apply the formulas we derive only over a range of variables such that the geometry is preserved. Then we have

$$\theta_1 = \beta \pm \psi, \tag{4.33}$$

where the plus sign is used if $\theta_2 < 0$ and the minus sign if $\theta_2 > 0$.

We know that angles in a plane add, so the sum of the three joint angles must be the orientation of the last link:

$$\theta_1 + \theta_2 + \theta_3 = \phi. \tag{4.34}$$

This equation is solved for θ_3 to complete our solution.

4.5 ALGEBRAIC SOLUTION BY REDUCTION TO POLYNOMIAL

Transcendental equations are often difficult to solve because, even when there is only one variable (say, θ), it generally appears as $\sin\theta$ and $\cos\theta$. Making the following substitutions, however, yields an expression in terms of a single variable, u:

$$\begin{aligned} u &= \tan\frac{\theta}{2}, \\ \cos\theta &= \frac{1 - u^2}{1 + u^2}, \\ \sin\theta &= \frac{2u}{1 + u^2}. \end{aligned} \tag{4.35}$$

This is a very important geometric substitution used often in solving kinematic equations. These substitutions convert transcendental equations into polynomial equations in u. Appendix A lists these and other trigonometric identities.

EXAMPLE 4.3

Convert the transcendental equation

$$a\cos\theta + b\sin\theta = c \tag{4.36}$$

into a polynomial in the tangent of the half angle, and solve for θ.

Substituting from (4.35) and multiplying through by $1 + u^2$, we have

$$a(1 - u^2) + 2bu = c(1 + u^2). \tag{4.37}$$

Collecting powers of u yields

$$(a + c)u^2 - 2bu + (c - a) = 0, \tag{4.38}$$

which is solved by the quadratic formula:

$$u = \frac{b \pm \sqrt{b^2 + a^2 - c^2}}{a + c}. \tag{4.39}$$

Hence,

$$\theta = 2\tan^{-1}\left(\frac{b \pm \sqrt{b^2 + a^2 - c^2}}{a + c}\right). \tag{4.40}$$

Should the solution for u from (4.39) be complex, there is no real solution to the original transcendental equation. Note that, if $a + c = 0$, the argument of the arctangent becomes infinity and hence $\theta = 180°$. In a computer implementation, this potential division by zero should be checked for ahead of time. This situation results when the quadratic term of (4.38) vanishes, so that the quadratic degenerates into a linear equation.

Polynomials up to degree four possess closed-form solutions [8, 9], so manipulators sufficiently simple that they can be solved by algebraic equations of this degree (or lower) are called **closed-form-solvable** manipulators.

4.6 PIEPER'S SOLUTION WHEN THREE AXES INTERSECT

As mentioned earlier, although a completely general robot with six degrees of freedom does not have a closed-form solution, certain important special cases can be solved. Pieper [3, 4] studied manipulators with six degrees of freedom in which three consecutive axes intersect at a point.[2] In this section, we outline the method he developed for the case of all six joints revolute, with the last three axes intersecting. His method applies to other configurations, which include prismatic

[2]Included in this family of manipulators are those with three consecutive parallel axes, because they meet at the point at infinity.

joints, and the interested reader should see [4]. Pieper's work applies to the majority of commercially available industrial robots.

When the last three axes intersect, the origins of link frames {4}, {5}, and {6} are all located at this point of intersection. This point is given in base coordinates as

$$ {}^0P_{4ORG} = {}^0_1T\,{}^1_2T\,{}^2_3T\,{}^3P_{4ORG} = \begin{bmatrix} x \\ y \\ z \\ 1 \end{bmatrix}, \tag{4.41} $$

or, using the fourth column of (3.6) for $i = 4$, as

$$ {}^0P_{4ORG} = {}^0_1T\,{}^1_2T\,{}^2_3T \begin{bmatrix} a_3 \\ -d_4 s\alpha_3 \\ d_4 c\alpha_3 \\ 1 \end{bmatrix}, \tag{4.42} $$

or as

$$ {}^0P_{4ORG} = {}^0_1T\,{}^1_2T \begin{bmatrix} f_1(\theta_3) \\ f_2(\theta_3) \\ f_3(\theta_3) \\ 1 \end{bmatrix}, \tag{4.43} $$

where

$$ \begin{bmatrix} f_1 \\ f_2 \\ f_3 \\ 1 \end{bmatrix} = {}^2_3T \begin{bmatrix} a_3 \\ -d_4 s\alpha_3 \\ d_4 c\alpha_3 \\ 1 \end{bmatrix}. \tag{4.44} $$

Using (3.6) for ${}^2_3T$ in (4.44) yields the following expressions for f_1:

$$ \begin{aligned} f_1 &= a_3c_3 + d_4s\alpha_3s_3 + a_2, \\ f_2 &= a_3c\alpha_2s_3 - d_4s\alpha_3c\alpha_2c_3 - d_4s\alpha_2c\alpha_3 - d_3s\alpha_2, \\ f_3 &= a_3s\alpha_2s_3 - d_4s\alpha_3s\alpha_2c_3 + d_4c\alpha_2c\alpha_3 + d_3c\alpha_2. \end{aligned} \tag{4.45} $$

Using (3.6) for ${}^0_1T$ and ${}^1_2T$ in (4.43), we obtain

$$ {}^0P_{4ORG} = \begin{bmatrix} c_1g_1 - s_1g_2 \\ s_1g_1 + c_1g_2 \\ g_3 \\ 1 \end{bmatrix}, \tag{4.46} $$

where

$$ \begin{aligned} g_1 &= c_2f_1 - s_2f_2 + a_1, \\ g_2 &= s_2c\alpha_1f_1 + c_2c\alpha_1f_2 - s\alpha_1f_3 - d_2s\alpha_1, \\ g_3 &= s_2s\alpha_1f_1 + c_2s\alpha_1f_2 + c\alpha_1f_3 + d_2c\alpha_1. \end{aligned} \tag{4.47} $$

We now write an expression for the squared magnitude of ${}^0P_{4ORG}$, which we will denote as $r = x^2 + y^2 + z^2$, and which is seen from (4.46) to be

$$ r = g_1^2 + g_2^2 + g_3^2; \tag{4.48} $$

so, using (4.47) for the g_i, we have

$$r = f_1^2 + f_2^2 + f_3^2 + a_1^2 + d_2^2 + 2d_2 f_3 + 2a_1(c_2 f_1 - s_2 f_2). \tag{4.49}$$

We now write this equation, along with the Z-component equation from (4.46), as a system of two equations in the form

$$\begin{aligned} r &= (k_1 c_2 + k_2 s_2)2a_1 + k_3, \\ z &= (k_1 s_2 - k_2 c_2)s\alpha_1 + k_4, \end{aligned} \tag{4.50}$$

where

$$\begin{aligned} k_1 &= f_1, \\ k_2 &= -f_2, \\ k_3 &= f_1^2 + f_2^2 + f_3^2 + a_1^2 + d_2^2 + 2d_2 f_3, \\ k_4 &= f_3 c\alpha_1 + d_2 c\alpha_1. \end{aligned} \tag{4.51}$$

Equation (4.50) is useful because dependence on θ_1 has been eliminated and because dependence on θ_2 takes a simple form.

Now let us consider the solution of (4.50) for θ_3. We distinguish three cases:

1. If $a_1 = 0$, then we have $r = k_3$, where r is known. The right-hand side (k_3) is a function of θ_3 only. After the substitution (4.35), a quadratic equation in $\tan\frac{\theta_3}{2}$ may be solved for θ_3.
2. If $s\alpha_1 = 0$, then we have $z = k_4$, where z is known. Again, after substituting via (4.35), a quadratic equation arises that can be solved for θ_3.
3. Otherwise, eliminate s_2 and c_2 from (4.50) to obtain

$$\frac{(r - k_3)^2}{4a_1^2} + \frac{(z - k_4)^2}{s^2\alpha_1} = k_1^2 + k_2^2. \tag{4.52}$$

This equation, after the (4.35) substitution for θ_3, results in an equation of degree 4, which can be solved for θ_3.[3]

Having solved for θ_3, we can solve (4.50) for θ_2 and (4.46) for θ_1.

To complete our solution, we need to solve for θ_4, θ_5, and θ_6. These axes intersect, so these joint angles affect the orientation of only the last link. We can compute them from nothing more than the rotation portion of the specified goal, ${}^0_6R$. Having obtained θ_1, θ_2, and θ_3, we can compute ${}^0_4R|_{\theta_4=0}$, by which notation we mean the orientation of link frame {4} relative to the base frame when $\theta_4 = 0$. The desired orientation of {6} differs from this orientation only by the action of the last three joints. Because the problem was specified as given ${}^0_6R$, we can compute

$${}^4_6R|_{\theta_4=0} = {}^0_4R^{-1}|_{\theta_4=0}\,{}^0_6R. \tag{4.53}$$

[3]It is helpful to note that $f_1^2 + f_2^2 + f_3^2 = a_3^2 + d_4^2 + d_3^2 + a_2^2 + 2d_4 d_3 c\alpha_3 + 2a_2 a_3 c_3 + 2a_2 d_4 s\alpha_3 s_3$.

For many manipulators, these last three angles can be solved for by using exactly the Z–Y–Z Euler angle solution given in Chapter 2, applied to ${}^4_6R|_{\theta_4=0}$. For any manipulator (with intersecting axes 4, 5, and 6), the last three joint angles can be solved for as a set of appropriately defined Euler angles. There are always two solutions for these last three joints, so the total number of solutions for the manipulator will be twice the number found for the first three joints.

4.7 EXAMPLES OF INVERSE MANIPULATOR KINEMATICS

In this section, we work out the inverse kinematics of two industrial robots. One manipulator solution is done purely algebraically; the second solution is partially algebraic and partially geometric. The following solutions do not constitute a cookbook method of solving manipulator kinematics, but they do show many of the common manipulations likely to appear in most kinematic solutions. Note that Pieper's method of solution (covered in the preceding section) can be used for these manipulators, but here we choose to approach the solution a different way, to give insight into various available methods.

The Unimation PUMA 560

As an example of the algebraic solution technique applied to a manipulator with six degrees of freedom, we will solve the kinematic equations of the PUMA 560, which were developed in Chapter 3. This solution is in the style of [5].

We wish to solve

$$
\begin{aligned}
{}^0_6T &= \begin{bmatrix} r_{11} & r_{12} & r_{13} & p_x \\ r_{21} & r_{22} & r_{23} & p_y \\ r_{31} & r_{32} & r_{33} & p_z \\ 0 & 0 & 0 & 1 \end{bmatrix} \\
&= {}^0_1T(\theta_1)\,{}^1_2T(\theta_2)\,{}^2_3T(\theta_3)\,{}^3_4T(\theta_4)\,{}^4_5T(\theta_5)\,{}^5_6T(\theta_6)
\end{aligned}
\tag{4.54}
$$

for θ_i when ${}^0_6T$ is given as numeric values.

A restatement of (4.54) that puts the dependence on θ_1 on the left-hand side of the equation is

$$
[{}^0_1T(\theta_1)]^{-1}\,{}^0_6T = {}^1_2T(\theta_2)\,{}^2_3T(\theta_3)\,{}^3_4T(\theta_4)\,{}^4_5T(\theta_5)\,{}^5_6T(\theta_6). \tag{4.55}
$$

Inverting ${}^0_1T$, we write (4.55) as

$$
\begin{bmatrix} c_1 & s_1 & 0 & 0 \\ -s_1 & c_1 & 0 & 0 \\ 0 & 0 & 1 & 0 \\ 0 & 0 & 0 & 1 \end{bmatrix}
\begin{bmatrix} r_{11} & r_{12} & r_{13} & p_x \\ r_{21} & r_{22} & r_{23} & p_y \\ r_{31} & r_{32} & r_{33} & p_z \\ 0 & 0 & 0 & 1 \end{bmatrix}
= {}^1_6T, \tag{4.56}
$$

where ${}^1_6T$ is given by equation (3.13) developed in Chapter 3. This simple technique of multiplying each side of a transform equation by an inverse is often used to advantage in separating out variables in the search for a solvable equation.

Equating the (2, 4) elements from both sides of (4.56), we have

$$
-s_1p_x + c_1p_y = d_3. \tag{4.57}
$$

To solve an equation of this form, we make the trigonometric substitutions

$$\begin{aligned} p_x &= \rho \cos\phi, \\ p_y &= \rho \sin\phi, \end{aligned} \tag{4.58}$$

where

$$\begin{aligned} \rho &= \sqrt{p_x^2 + p_y^2}, \\ \phi &= \text{Atan2}(p_y, p_x). \end{aligned} \tag{4.59}$$

Substituting (4.58) into (4.57), we obtain

$$c_1 s_\phi - s_1 c_\phi = \frac{d_3}{\rho}. \tag{4.60}$$

From the difference-of-angles formula,

$$\sin(\phi - \theta_1) = \frac{d_3}{\rho}. \tag{4.61}$$

Hence,

$$\cos(\phi - \theta_1) = \pm\sqrt{1 - \frac{d_3^2}{\rho^2}}, \tag{4.62}$$

and so

$$\phi - \theta_1 = \text{Atan2}\left(\frac{d_3}{\rho}, \pm\sqrt{1 - \frac{d_3^2}{\rho^2}}\right). \tag{4.63}$$

Finally, the solution for θ_1 may be written as

$$\theta_1 = \text{Atan2}(p_y, p_x) - \text{Atan2}\left(d_3, \pm\sqrt{p_x^2 + p_y^2 - d_3^2}\right). \tag{4.64}$$

Note that we have found two possible solutions for θ_1, corresponding to the plus-or-minus sign in (4.64). Now that θ_1 is known, the left-hand side of (4.56) is known. If we equate both the (1,4) elements and the (3,4) elements from the two sides of (4.56), we obtain

$$\begin{aligned} c_1 p_x + s_1 p_y &= a_3 c_{23} - d_4 s_{23} + a_2 c_2, \\ -p_x &= a_3 s_{23} + d_4 c_{23} + a_2 s_2. \end{aligned} \tag{4.65}$$

If we square equations (4.65) and (4.57) and add the resulting equations, we obtain

$$a_3 c_3 - d_4 s_3 = K, \tag{4.66}$$

where

$$K = \frac{p_x^2 + p_y^2 + p_x^2 - a_2^2 - a_3^2 - d_3^2 - d_4^2}{2a_2}. \tag{4.67}$$

Note that dependence on θ_1 has been removed from (4.66). Equation (4.66) is of the same form as (4.57) and so can be solved by the same kind of trigonometric substitution to yield a solution for θ_3:

$$\theta_3 = \text{Atan2}(a_3, d_4) - \text{Atan2}(K, \pm\sqrt{a_3^2 + d_4^2 - K^2}). \tag{4.68}$$

The plus-or-minus sign in (4.68) leads to two different solutions for θ_3. If we consider (4.54) again, we can now rewrite it so that all the left-hand side is a function of only knowns and θ_2:

$$[{}^0_3T(\theta_2)]^{-1}{}^0_6T = {}^3_4T(\theta_4){}^4_5T(\theta_5){}^5_6T(\theta_6), \tag{4.69}$$

or

$$\begin{bmatrix} c_1c_{23} & s_1c_{23} & -s_{23} & -a_2c_3 \\ -c_1s_{23} & -s_1s_{23} & -c_{23} & a_2s_3 \\ -s_1 & c_1 & 0 & -d_3 \\ 0 & 0 & 0 & 1 \end{bmatrix} \begin{bmatrix} r_{11} & r_{12} & r_{13} & p_x \\ r_{21} & r_{22} & r_{23} & p_y \\ r_{31} & r_{32} & r_{33} & p_z \\ 0 & 0 & 0 & 1 \end{bmatrix} = {}^3_6T, \tag{4.70}$$

where ${}^3_6T$ is given by equation (3.11) developed in Chapter 3. Equating both the (1,4) elements and the (2,4) elements from the two sides of (4.70), we get

$$\begin{aligned} c_1c_{23}p_x + s_1c_{23}p_y - s_{23}p_z - a_2c_3 &= a_3, \\ -c_1s_{23}p_x - s_1s_{23}p_y - c_{23}p_z + a_2s_3 &= d_4. \end{aligned} \tag{4.71}$$

These equations can be solved simultaneously for s_{23} and c_{23}, resulting in

$$\begin{aligned} s_{23} &= \frac{(-a_3 - a_2c_3)p_z + (c_1p_x + s_1p_y)(a_2s_3 - d_4)}{p_z^2 + (c_1p_x + s_1p_y)^2}, \\ c_{23} &= \frac{(a_2s_3 - d_4)p_z - (a_3 + a_2c_3)(c_1p_x + s_1p_y)}{p_z^2 + (c_1p_x + s_1p_y)^2}. \end{aligned} \tag{4.72}$$

The denominators are equal and positive, so we solve for the sum of θ_2 and θ_3 as

$$\begin{aligned} \theta_{23} = \text{Atan2}[&(-a_3 - a_2c_3)p_z - (c_1p_x + s_1p_y)(d_4 - a_2s_3), \\ &(a_2s_3 - d_4)p_z - (a_3 + a_2c_3)(c_1p_x + s_1p_y)]. \end{aligned} \tag{4.73}$$

Equation (4.73) computes four values of θ_{23}, according to the four possible combinations of solutions for θ_1 and θ_3; then, four possible solutions for θ_2 are computed as

$$\theta_2 = \theta_{23} - \theta_3, \tag{4.74}$$

where the appropriate solution for θ_3 is used when forming the difference.

Now the entire left side of (4.70) is known. Equating both the (1,3) elements and the (3,3) elements from the two sides of (4.70), we get

$$\begin{aligned} r_{13}c_1c_{23} + r_{23}s_1c_{23} - r_{33}s_{23} &= -c_4s_5, \\ -r_{13}s_1 + r_{23}c_1 &= s_4s_5. \end{aligned} \tag{4.75}$$

As long as $s_5 \neq 0$, we can solve for θ_4 as

$$\theta_4 = \text{Atan2}(-r_{13}s_1 + r_{23}c_1, -r_{13}c_1c_{23} - r_{23}s_1c_{23} + r_{33}s_{23}). \tag{4.76}$$

When $\theta_5 = 0$, the manipulator is in a singular configuration in which joint axes 4 and 6 line up and cause the same motion of the last link of the robot. In this case, all that matters (and all that can be solved for) is the sum or difference of θ_4 and θ_6. This situation is detected by checking whether both arguments of the Atan2 in (4.76) are near zero. If so, θ_4 is chosen arbitrarily,[4] and when θ_6 is computed later, it will be computed accordingly.

If we consider (4.54) again, we can now rewrite it so that all the left-hand side is a function of only knowns and θ_4, by rewriting it as

$$[{}^0_4T(\theta_4)]^{-1}\,{}^0_6T = {}^4_5T(\theta_5){}^5_6T(\theta_6), \tag{4.77}$$

where $[{}^0_4T(\theta 4)]^{-1}$ is given by

$$\begin{bmatrix} c_1c_{23}c_4 + s_1s_4 & s_1c_{23}c_4 - c_1s_4 & -s_{23}c_4 & -a_2c_3c_4 + d_3s_4 - a_3c_4 \\ -c_1c_{23}s_4 + s_1c_4 & -s_1c_{23}s_4 - c_1c_4 & s_{23}s_4 & a_2c_3s_4 + d_3c_4 + a_3s_4 \\ -c_1s_{23} & -s_1s_{23} & -c_{23} & a_2s_3 - d_4 \\ 0 & 0 & 0 & 1 \end{bmatrix}, \tag{4.78}$$

and ${}^4_6T$ is given by equation (3.10) developed in Chapter 3. Equating both the (1,3) elements and the (3,3) elements from the two sides of (4.77), we get

$$\begin{aligned} r_{13}(c_1c_{23}c_4 + s_1s_4) + r_{23}(s_1c_{23}c_4 - c_1s_4) - r_{33}(s_{23}c_4) &= -s_5, \\ r_{13}(-c_1s_{23}) + r_{23}(-s_1s_{23}) + r_{33}(-c_{23}) &= c_5. \end{aligned} \tag{4.79}$$

Hence, we can solve for θ_5 as

$$\theta_5 = \text{Atan2}(s_5, c_5), \tag{4.80}$$

where s_5 and c_5 are given by (4.79).

Applying the same method one more time, we compute $({}^0_5T)^{-1}$ and write (4.54) in the form

$$({}^0_5T)^{-1}\,{}^0_6T = {}^5_6T(\theta_6). \tag{4.81}$$

Equating both the (3,1) elements and the (1,1) elements from the two sides of (4.77) as we have done before, we get

$$\theta_6 = \text{Atan2}(s_6, c_6), \tag{4.82}$$

where

$$\begin{aligned} s_6 &= -r_{11}(c_1c_{23}s_4 - s_1c_4) - r_{21}(s_1c_{23}s_4 + c_1c_4) + r_{31}(s_{23}s_4), \\ c_6 &= r_{11}[(c_1c_{23}c_4 + s_1s_4)c_5 - c_1s_{23}s_5] + r_{21}[(s_1c_{23}c_4 - c_1s_4)c_5 - s_1s_{23}s_5] \\ &\quad -r_{31}(s_{23}c_4c_5 + c_{23}s_5). \end{aligned}$$

Because of the plus-or-minus signs appearing in (4.64) and (4.68), these equations compute four solutions. Additionally, there are four more solutions obtained by

[4] It is usually chosen to be equal to the present value of joint 4.

"flipping" the wrist of the manipulator. For each of the four solutions computed above, we obtain the flipped solution by

$$\begin{aligned} \theta_4' &= \theta_4 + 180°, \\ \theta_5' &= -\theta_5, \\ \theta_6' &= \theta_6 + 180°. \end{aligned} \tag{4.83}$$

After all eight solutions have been computed, some (or even all) of them might have to be discarded because of joint-limit violations. Of any remaining valid solutions, usually the one closest to the present manipulator configuration is chosen.

The Yasukawa Motoman L-3

As the second example, we will solve the kinematic equations of the Yasukawa Motoman L-3, which were developed in Chapter 3. This solution will be partially algebraic and partially geometric. The Motoman L-3 has three features that make the inverse kinematic problem quite different from that of the PUMA. First, the manipulator has only five joints, so it is not able to position and orient its end-effector in order to attain *general* goal frames. Second, the four-bar type of linkages and chain-drive scheme cause one actuator to move two or more joints. Third, the actuator position limits are not constants, but depend on the positions of the other actuators, so finding out whether a computed set of actuator values is in range is not trivial.

If we consider the nature of the subspace of the Motoman manipulator (and the same applies to many manipulators with five degrees of freedom), we quickly realize that this subspace can be described by giving one constraint on the attainable orientation: The pointing direction of the tool, that is, the $\hat{Z}_T$ axis, must lie in the "plane of the arm." This plane is the vertical plane that contains the axis of joint 1 and the point where axes 4 and 5 intersect. The orientation nearest to a general orientation is the one obtained by rotating the tool's pointing direction so that it lies in the plane, using a minimum amount of rotation. Without developing an explicit expression for this subspace, we will construct a method for projecting a general goal frame into it. Note that this entire discussion is for the case that the wrist frame and tool frame differ only by a translation along $\hat{Z}_w$.

In Fig. 4.9, we indicate the plane of the arm by its normal, $\hat{M}$, and the desired pointing direction of the tool by $\hat{Z}_T$. This pointing direction must be rotated by angle θ about some vector $\hat{K}$ in order to cause the new pointing direction, $\hat{Z}_T'$, to lie in the plane. It is clear that the $\hat{K}$ that minimizes θ lies in the plane and is orthogonal to both $\hat{Z}_T$ and $\hat{Z}_T'$.

For any given goal frame, $\hat{M}$ is defined as

$$\hat{M} = \frac{1}{\sqrt{p_x^2 + p_y^2}} \begin{bmatrix} -p_y \\ p_x \\ 0 \end{bmatrix}, \tag{4.84}$$

where p_x and p_y are the X and Y coordinates of the desired tool position. Then K is given by

$$K = \hat{M} \times \hat{Z}_T. \tag{4.85}$$

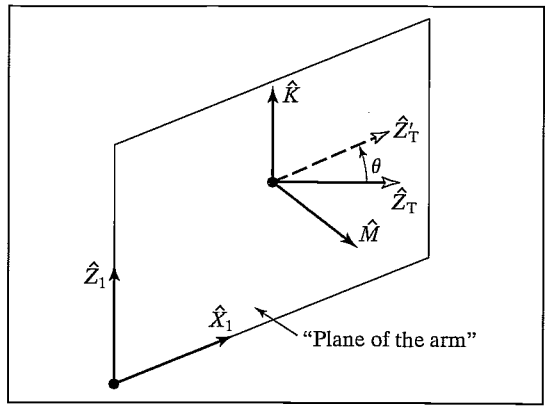

FIGURE 4.9: Rotating a goal frame into the Motoman's subspace.

The new $\hat{Z}'_T$ is

$$\hat{Z}'_T = \hat{K} \times \hat{M}. \tag{4.86}$$

The amount of rotation, θ, is given by

$$\begin{aligned} \cos\theta &= \hat{Z}_T \cdot \hat{Z}'_T, \\ \sin\theta &= (\hat{Z}_T \times \hat{Z}'_T) \cdot \hat{K}. \end{aligned} \tag{4.87}$$

Using Rodriques's formula (see Exercise 2.20), we have

$$\hat{Y}'_T = c\theta \hat{Y}_T + s\theta(\hat{K} \times \hat{Y}_T) + (1 - c\theta)(\hat{K} \cdot \hat{Y}_T)\hat{K}. \tag{4.88}$$

Finally, we compute the remaining unknown column of the new rotation matrix of the tool as

$$\hat{X}'_T = \hat{Y}'_T \times \hat{Z}'_T. \tag{4.89}$$

Equations (4.84) through (4.89) describe a method of projecting a given general goal orientation into the subspace of the Motoman robot.

Assuming that the given wrist frame, ${}^{B}_{W}T$, lies in the manipulator's subspace, we solve the kinematic equations as follows. In deriving the kinematic equations for the Motoman L-3, we formed the product of link transformations:

$${}^{0}_{5}T = {}^{0}_{1}T\,{}^{1}_{2}T\,{}^{2}_{3}T\,{}^{3}_{4}T\,{}^{4}_{5}T. \tag{4.90}$$

If we let

$${}^{0}_{5}T = \begin{bmatrix} r_{11} & r_{12} & r_{13} & p_x \\ r_{21} & r_{22} & r_{23} & p_y \\ r_{31} & r_{32} & r_{33} & p_z \\ 0 & 0 & 0 & 1 \end{bmatrix} \tag{4.91}$$

and premultiply both sides by ${}^{0}_{1}T^{-1}$, we have

$${}^{0}_{1}T^{-1}\,{}^{0}_{5}T = {}^{1}_{2}T\,{}^{2}_{3}T\,{}^{3}_{4}T\,{}^{4}_{5}T, \tag{4.92}$$

where the left-hand side is

$$\begin{bmatrix} c_1r_{11}+s_1r_{21} & c_1r_{12}+s_1r_{22} & c_1r_{13}+s_1r_{23} & c_1p_x+s_1p_y \\ -r_{31} & -r_{32} & -r_{33} & -p_z \\ -s_1r_{11}+c_1r_{21} & -s_1r_{12}+c_1r_{22} & -s_1r_{13}+c_1r_{23} & -s_1p_x+c_1p_y \\ 0 & 0 & 0 & 1 \end{bmatrix} \tag{4.93}$$

and the right-hand side is

$$\begin{bmatrix} * & * & s_{234} & * \\ * & * & -c_{234} & * \\ s_5 & c_5 & 0 & 0 \\ 0 & 0 & 0 & 1 \end{bmatrix}; \tag{4.94}$$

in the latter, several of the elements have not been shown. Equating the (3,4) elements, we get

$$-s_1p_x + c_1p_y = 0, \tag{4.95}$$

which gives us[5]

$$\theta_1 = \text{Atan2}(p_y, p_x). \tag{4.96}$$

Equating the (3,1) and (3,2) elements, we get

$$\begin{aligned} s_5 &= -s_1r_{11} + c_1r_{21}, \\ c_5 &= -s_1r_{12} + c_1r_{22}, \end{aligned} \tag{4.97}$$

from which we calculate θ_5 as

$$\theta_5 = \text{Atan2}(r_{21}c_1 - r_{11}s_1, r_{22}c_1 - r_{12}s_1). \tag{4.98}$$

Equating the (2,3) and (1,3) elements, we get

$$\begin{aligned} c_{234} &= r_{33}, \\ s_{234} &= c_1r_{13} + s_1r_{23}, \end{aligned} \tag{4.99}$$

which leads to

$$\theta_{234} = \text{Atan2}(r_{13}c_1 + r_{23}s_1, r_{33}). \tag{4.100}$$

To solve for the individual angles θ_2, θ_3, and θ_4, we will take a geometric approach. Figure 4.10 shows the plane of the arm with point A at joint axis 2, point B at joint axis 3, and point C at joint axis 4.

From the law of cosines applied to triangle ABC, we have

$$\cos\theta_3 = \frac{p_x^2 + p_y^2 + p_z^2 - l_2^2 - l_3^2}{2l_2l_3}. \tag{4.101}$$

Next, we have[6]

$$\theta_3 = \text{Atan2}\left(\sqrt{1-\cos^2\theta_3}, \cos\theta_3\right). \tag{4.102}$$

[5]For this manipulator, a second solution would violate joint limits and so is not calculated.

[6]For this manipulator, a second solution would violate joint limits and so is not calculated.

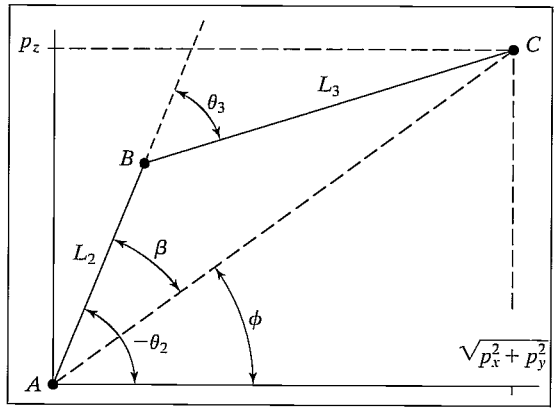

FIGURE 4.10: The plane of the Motoman manipulator.

From Fig. 4.10, we see that $\theta_2 = -\phi - \beta$, or

$$\theta_2 = -\text{Atan2}\left(p_z, \sqrt{p_x^2 + p_y^2}\right) - \text{Atan2}(l_3 \sin\theta_3, l_2 + l_3 \cos\theta_3). \tag{4.103}$$

Finally, we have

$$\theta_4 = \theta_{234} - \theta_2 - \theta_3. \tag{4.104}$$

Having solved for joint angles, we must perform the further computation to obtain the actuator values. Referring to Section 3.7, we solve equation (3.16) for the A_i:

$$\begin{aligned}
A_1 &= \frac{1}{k_1}(\theta_1 - \lambda_1), \\
A_2 &= \frac{1}{k_2}\left(\sqrt{-2\alpha_2\beta_2 \cos\left(\theta_2 - \Omega_2 - \tan^{-1}\left(\frac{\phi_2}{\gamma_2}\right) + 270^\circ\right) + \alpha_2^2 + \beta_2^2} - \lambda_2\right), \\
A_3 &= \frac{1}{k_3}\left(\sqrt{-2\alpha_3\beta_3 \cos\left(\theta_2 + \theta_3 - \tan^{-1}\left(\frac{\phi_3}{\gamma_3}\right) + 90^\circ\right) + \alpha_3^2 + \beta_3^2} - \lambda_3\right), \\
A_4 &= \frac{1}{k_4}(180^\circ + \lambda_4 - \theta_2 - \theta_3 - \theta_4), \\
A_5 &= \frac{1}{k_5}(\lambda_5 - \theta_5).
\end{aligned} \tag{4.105}$$

The actuators have limited ranges of motion, so we must check that our computed solution is in range. This "in range" check is complicated by the fact that the mechanical arrangement makes actuators interact and affect each other's allowed range of motion. For the Motoman robot, actuators 2 and 3 interact in such a way that the following relationship must always be obeyed:

$$A_2 - 10,000 > A_3 > A_2 + 3000. \tag{4.106}$$

That is, the limits of actuator 3 are a function of the position of actuator 2. Similarly,

$$32{,}000 - A_4 < A_5 < 55{,}000. \tag{4.107}$$

Now, one revolution of joint 5 corresponds to 25,600 actuator counts, so, when $A_4 > 2600$, there are two possible solutions for A_5. This is the only situation in which the Yasukawa Motoman L-3 has more than one solution.

4.8 THE STANDARD FRAMES

The ability to solve for joint angles is really the central element in many robot control systems. Again, consider the paradigm indicated in Fig. 4.11, which shows the standard frames.

The way these frames are used in a general robot system is as follows:

1. The user specifies to the system where the station frame is to be located. This might be at the corner of a work surface, as in Fig. 4.12, or even affixed to a moving conveyor belt. The station frame, $\{S\}$, is defined relative to the base frame, $\{B\}$.
2. The user specifies the description of the tool being used by the robot by giving the $\{T\}$-frame specification. Each tool the robot picks up could have a different $\{T\}$ frame associated with it. Note that the same tool grasped in different ways requires different $\{T\}$-frame definitions. $\{T\}$ is specified relative to $\{W\}$—that is, ${}^{W}_{T}T$.
3. The user specifies the goal point for a robot motion by giving the description of the goal frame, $\{G\}$, relative to the station frame. Often, the definitions of $\{T\}$ and $\{S\}$ remain fixed for several motions of the robot. In this case, once they are defined, the user simply gives a series of $\{G\}$ specifications.

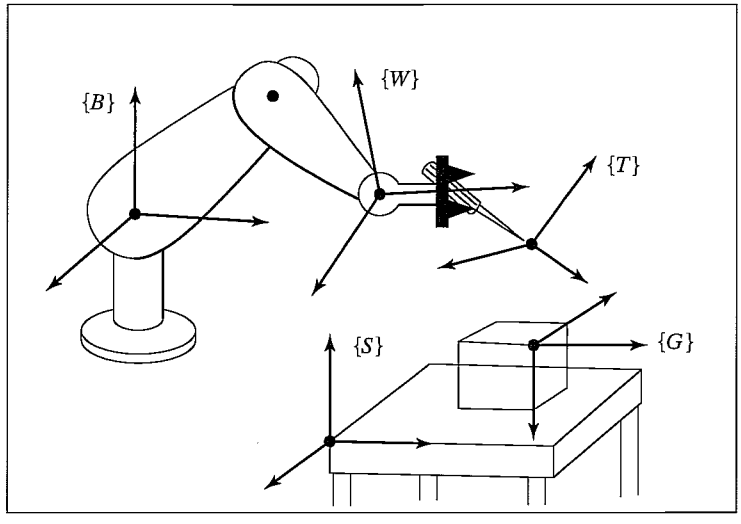

FIGURE 4.11: Location of the "standard" frames.

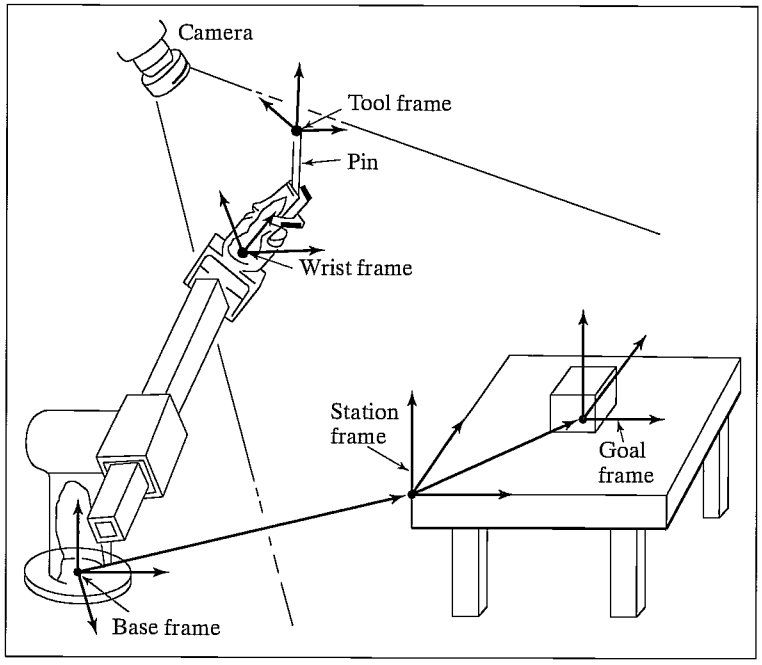

FIGURE 4.12: Example workstation.

In many systems, the tool frame definition (${}^{W}_{T}T$) is constant (for example, it is defined with its origin at the center of the fingertips). Also, the station frame might be fixed or might easily be taught by the user with the robot itself. In such systems, the user need not be aware of the five standard frames—he or she simply thinks in terms of moving the tool to locations (goals) with respect to the work area specified by station frame.

4. The robot system calculates a series of joint angles to move the joints through in order that the tool frame will move from its initial location in a smooth manner until $\{T\} = \{G\}$ at the end of motion.

4.9 SOLVE-ING A MANIPULATOR

The SOLVE function implements Cartesian transformations and calls the inverse kinematics function. Thus, the inverse kinematics are generalized so that arbitrary tool-frame and station-frame definitions may be used with our basic inverse kinematics, which solves for the wrist frame relative to the base frame.

Given the goal-frame specification, ${}^{S}_{T}T$, SOLVE uses the tool and station definitions to calculate the location of $\{W\}$ relative to $\{B\}$, ${}^{B}_{W}T$:

$$ {}^{B}_{W}T = {}^{B}_{S}T\,{}^{S}_{T}T\,{}^{W}_{T}T^{-1}. \tag{4.108} $$

Then, the inverse kinematics take ${}^{B}_{W}T$ as an input and calculate θ_1 through θ_n.

4.10 REPEATABILITY AND ACCURACY

Many industrial robots today move to goal points that have been taught. A **taught point** is one that the manipulator is moved to physically, and then the joint position sensors are read and the joint angles stored. When the robot is commanded to return to that point in space, each joint is moved to the stored value. In simple "teach and playback" manipulators such as these, the inverse kinematic problem never arises, because goal points are never specified in Cartesian coordinates. When a manufacturer specifies how precisely a manipulator can return to a taught point, he is specifying the **repeatability** of the manipulator.

Any time a goal position and orientation are specified in Cartesian terms, the inverse kinematics of the device must be computed in order to solve for the required joint angles. Systems that allow goals to be described in Cartesian terms are capable of moving the manipulator to points that were never taught—points in its workspace to which it has perhaps never gone before. We will call such points **computed points**. Such a capability is necessary for many manipulation tasks. For example, if a computer vision system is used to locate a part that the robot must grasp, the robot must be able to move to the Cartesian coordinates supplied by the vision sensor. The precision with which a computed point can be attained is called the **accuracy** of the manipulator.

The accuracy of a manipulator is bounded by the repeatability. Clearly, accuracy is affected by the precision of parameters appearing in the kinematic equations of the robot. Errors in knowledge of the Denavit–Hartenberg parameters will cause the inverse kinematic equations to calculate joint angle values that are in error. Hence, although the repeatability of most industrial manipulators is quite good, the accuracy is usually much worse and varies quite a bit from manipulator to manipulator. Calibration techniques can be devised that allow the accuracy of a manipulator to be improved through estimation of that particular manipulator's kinematic parameters [10].

4.11 COMPUTATIONAL CONSIDERATIONS

In many path-control schemes, which we will consider in Chapter 7, it is necessary to calculate the inverse kinematics of a manipulator at fairly high rates, for example, 30 Hz or faster. Therefore, computational efficiency is an issue. These speed requirements rule out the use of numerical-solution techniques that are iterative in nature; for this reason, we have not considered them.

Most of the general comments of Section 3.10, made for forward kinematics, also hold for the problem of inverse kinematics. For the inverse-kinematic case, a table-lookup Atan2 routine is often used to attain higher speeds.

Structure of the computation of multiple solutions is also important. It is generally fairly efficient to generate all of them in parallel, rather than pursuing one after another serially. Of course, in some applications, when all solutions are not required, substantial time is saved by computing only one.

When a geometric approach is used to develop an inverse-kinematic solution, it is sometimes possible to calculate multiple solutions by simple operations on the various angles solved for in obtaining the first solution. That is, the first solution

is moderately expensive computationally, but the other solutions are found very quickly by summing and differencing angles, subtracting π, and so on.

BIBLIOGRAPHY

[1] B. Roth, J. Rastegar, and V. Scheinman, "On the Design of Computer Controlled Manipulators," *On the Theory and Practice of Robots and Manipulators*, Vol. 1, First CISM-IFToMM Symposium, September 1973, pp. 93–113.

[2] B. Roth, "Performance Evaluation of Manipulators from a Kinematic Viewpoint," *Performance Evaluation of Manipulators*, National Bureau of Standards, special publication, 1975.

[3] D. Pieper and B. Roth, "The Kinematics of Manipulators Under Computer Control," *Proceedings of the Second International Congress on Theory of Machines and Mechanisms*, Vol. 2, Zakopane, Poland, 1969, pp. 159–169.

[4] D. Pieper, "The Kinematics of Manipulators Under Computer Control," Unpublished Ph.D. Thesis, Stanford University, 1968.

[5] R.P. Paul, B. Shimano, and G. Mayer, "Kinematic Control Equations for Simple Manipulators," *IEEE Transactions on Systems, Man, and Cybernetics*, Vol. SMC-11, No. 6, 1981.

[6] L. Tsai and A. Morgan, "Solving the Kinematics of the Most General Six- and Five-degree-of-freedom Manipulators by Continuation Methods," Paper 84-DET-20, ASME Mechanisms Conference, Boston, October 7–10, 1984.

[7] C.S.G. Lee and M. Ziegler, "Geometric Approach in Solving Inverse Kinematics of PUMA Robots," *IEEE Transactions on Aerospace and Electronic Systems*, Vol. AES-20, No. 6, November 1984.

[8] W. Beyer, *CRC Standard Mathematical Tables*, 25th edition, CRC Press, Inc., Boca Raton, FL, 1980.

[9] R. Burington, *Handbook of Mathematical Tables and Formulas*, 5th edition, McGraw-Hill, New York, 1973.

[10] J. Hollerbach, "A Survey of Kinematic Calibration," in *The Robotics Review*, O. Khatib, J. Craig, and T. Lozano-Perez, Editors, MIT Press, Cambridge, MA, 1989.

[11] Y. Nakamura and H. Hanafusa, "Inverse Kinematic Solutions with Singularity Robustness for Robot Manipulator Control," *ASME Journal of Dynamic Systems, Measurement, and Control*, Vol. 108, 1986.

[12] D. Baker and C. Wampler, "On the Inverse Kinematics of Redundant Manipulators," *International Journal of Robotics Research*, Vol. 7, No. 2, 1988.

[13] L.W. Tsai, *Robot Analysis: The Mechanics of Serial and Parallel Manipulators*, Wiley, New York, 1999.

EXERCISES

4.1 [15] Sketch the fingertip workspace of the three-link manipulator of Chapter 3, Exercise 3.3 for the case $l_1 = 15.0$, $l_2 = 10.0$, and $l_3 = 3.0$.

4.2 [26] Derive the inverse kinematics of the three-link manipulator of Chapter 3, Exercise 3.3.

4.3 [12] Sketch the fingertip workspace of the 3-DOF manipulator of Chapter 3, Example 3.4.

4.4 [24] Derive the inverse kinematics of the 3-DOF manipulator of Chapter 3, Example 3.4.

4.5 [38] Write a Pascal (or C) subroutine that computes all possible solutions for the PUMA 560 manipulator that lie within the following joint limits:

$$\begin{aligned} -170.0 &< \theta_1 < 170.0, \\ -225.0 &< \theta_2 < 45.0, \\ -250.0 &< \theta_3 < 75.0, \\ -135.0 &< \theta_4 < 135.0, \\ -100.0 &< \theta_5 < 100.0, \\ -180.0 &< \theta_6 < 180.0. \end{aligned}$$

Use the equations derived in Section 4.7 with these numerical values (in inches):

$$\begin{aligned} a_2 &= 17.0, \\ a_3 &= 0.8, \\ d_3 &= 4.9, \\ d_4 &= 17.0. \end{aligned}$$

4.6 [15] Describe a simple algorithm for choosing the nearest solution from a set of possible solutions.

4.7 [10] Make a list of factors that might affect the repeatability of a manipulator. Make a second list of additional factors that affect the accuracy of a manipulator.

4.8 [12] Given a desired position and orientation of the hand of a three-link planar rotary-jointed manipulator, there are two possible solutions. If we add one more rotational joint (in such a way that the arm is still planar), how many solutions are there?

4.9 [26] Figure 4.13 shows a two-link planar arm with rotary joints. For this arm, the second link is half as long as the first—that is, $l_1 = 2l_2$. The joint range limits in

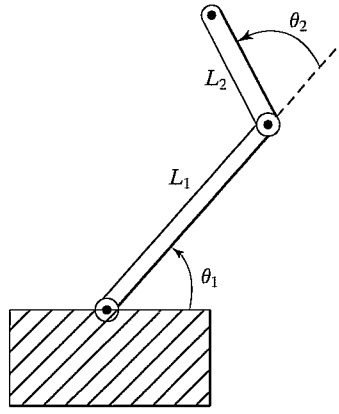

FIGURE 4.13: Two-link planar manipulator.

degrees are

$$0 < \theta_1 < 180,$$
$$-90 < \theta_2 < 180.$$

Sketch the approximate reachable workspace (an area) of the tip of link 2.

4.10 [23] Give an expression for the subspace of the manipulator of Chapter 3, Example 3.4.

4.11 [24] A 2-DOF positioning table is used to orient parts for arc-welding. The forward kinematics that locate the bed of the table (link 2) with respect to the base (link 0) are

$${}^0_2T = \begin{bmatrix} c_1c_2 & -c_1s_2 & s_1 & l_2s_1 + l_1 \\ s_2 & c_2 & 0 & 0 \\ -s_1c_2 & s_1s_2 & c_1 & l_2c_1 + h_1 \\ 0 & 0 & 0 & 1 \end{bmatrix}.$$

Given any unit direction fixed in the frame of the bed (link 2), ${}^2\hat{V}$, give the inverse-kinematic solution for θ_1, θ_2 such that this vector is aligned with ${}^0\hat{Z}$ (i.e., upward). Are there multiple solutions? Is there a singular condition for which a unique solution cannot be obtained?

4.12 [22] In Fig. 4.14, two $3R$ mechanisms are pictured. In both cases, the three axes intersect at a point (and, over all configurations, this point remains fixed in space). The mechanism in Fig. 4.14(a) has link twists (α_i) of magnitude 90 degrees. The mechanism in Fig. 4.14(b) has one twist of ϕ in magnitude and the other of $180 - \phi$ in magnitude.

The mechanism in Fig. 4.14(a) can be seen to be in correspondence with Z–Y–Z Euler angles, and therefore we know that it suffices to orient link 3 (with arrow in figure) arbitrarily with respect to the fixed link 0. Because ϕ is not equal to 90 degrees, it turns out that the other mechanism cannot orient link 3 arbitrarily.

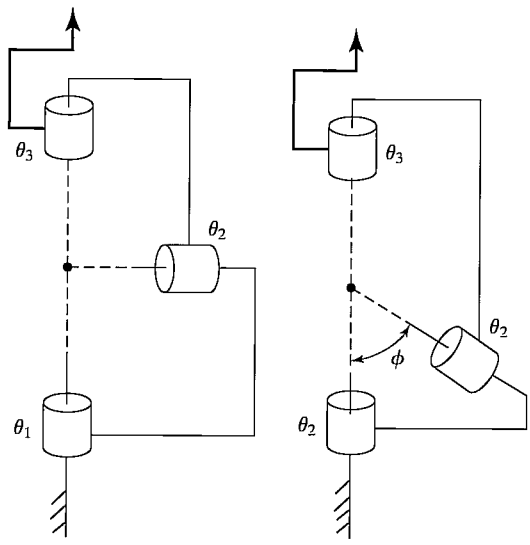

FIGURE 4.14: Two $3R$ mechanisms (Exercise 4.12).

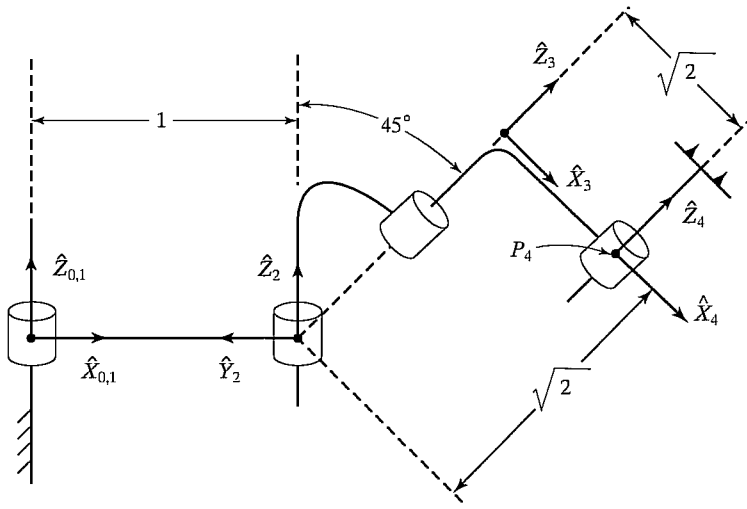

FIGURE 4.15: A $4R$ manipulator shown in the position $\Theta = [0, 90°, -90°, 0]^T$ (Exercise 4.16).

Describe the set of orientations that are *unattainable* with the second mechanism. Note that we assume that all joints can turn 360 degrees (i.e. no limits) and we assume that the links may pass through each other if need be (i.e., workspace not limited by self-collisions).

4.13 [13] Name two reasons for which closed-form analytic kinematic solutions are preferred over iterative solutions.

4.14 [14] There exist 6-DOF robots for which the kinematics are NOT closed-form solvable. Does there exist any 3-DOF robot for which the (position) kinematics are NOT closed-form solvable?

4.15 [38] Write a subroutine that solves quartic equations in closed form. (See [8, 9].)

4.16 [25] A $4R$ manipulator is shown schematically in Fig. 4.15. The nonzero link parameters are $a_1 = 1$, $\alpha_2 = 45°$, $d_3 = \sqrt{2}$, and $a_3 = \sqrt{2}$, and the mechanism is pictured in the configuration corresponding to $\Theta = [0, 90°, -90°, 0]^T$. Each joint has $\pm 180°$ as limits. Find all values of θ_3 such that

$$^0P_{4ORG} = [1.1, 1.5, 1.707]^T.$$

4.17 [25] A $4R$ manipulator is shown schematically in Fig. 4.16. The nonzero link parameters are $\alpha_1 = -90°$, $d_2 = 1$, $\alpha_2 = 45°$, $d_3 = 1$, and $a_3 = 1$, and the mechanism is pictured in the configuration corresponding to $\Theta = [0, 0, 90°, 0]^T$. Each joint has $\pm 180°$ as limits. Find all values of θ_3 such that

$$^0P_{4ORG} = [0.0, 1.0, 1.414]^T.$$

4.18 [15] Consider the RRP manipulator shown in Fig. 3.37. How many solutions do the (position) kinematic equations possess?

4.19 [15] Consider the RRR manipulator shown in Fig. 3.38. How many solutions do the (position) kinematic equations possess?

4.20 [15] Consider the RPP manipulator shown in Fig. 3.39. How many solutions do the (position) kinematic equations possess?

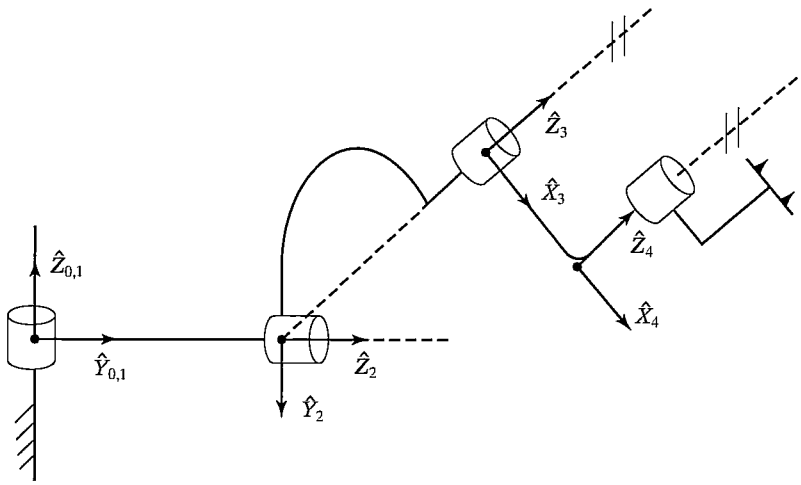

FIGURE 4.16: A $4R$ manipulator shown in the position $\Theta = [0, 0, 90°, 0]^T$ (Exercise 4.17).

4.21 [15] Consider the *PRR* manipulator shown in Fig. 3.40. How many solutions do the (position) kinematic equations possess?

4.22 [15] Consider the *PPP* manipulator shown in Fig. 3.41. How many solutions do the (position) kinematic equations possess?

4.23 [38] The following kinematic equations arise in a certain problem:

$$\begin{aligned} \sin\xi &= a\sin\theta + b, \\ \sin\phi &= c\cos\theta + d, \\ \psi &= \xi + \phi. \end{aligned}$$

Given a, b, c, d, and ψ, show that, in the general case, there are four solutions for θ. Give a special condition under which there are just two solutions for θ.

4.24 [20] Given the description of link frame $\{i\}$ in terms of link frame $\{i-1\}$, find the four Denavit–Hartenberg parameters as functions of the elements of ${}^{i-1}_{i}T$.

PROGRAMMING EXERCISE (PART 4)

1. Write a subroutine to calculate the inverse kinematics for the three-link manipulator of Section 4.4. The routine should pass arguments in the form

```
Procedure INVKIN(VAR wrelb: frame; VAR current, near, far: vec3;
VAR sol: boolean);
```

where "wrelb," an input, is the wrist frame specified relative to the base frame; "current," an input, is the current position of the robot (given as a vector of joint angles); "near" is the nearest solution; "far" is the second solution; and "sol" is a flag that indicates whether solutions were found. (sol = FALSE if no solutions were found). The link lengths (meters) are

$$l_1 = l_2 = 0.5.$$

The joint ranges of motion are

$$-170^\circ \leq \theta_i \leq 170^\circ.$$

Test your routine by calling it back-to-back with KIN to demonstrate that they are indeed inverses of one another.

2. A tool is attached to link 3 of the manipulator. This tool is described by ${}^{W}_{T}T$, the tool frame relative to the wrist frame. Also, a user has described his work area, the station frame relative to the base of the robot, as ${}^{B}_{S}T$. Write the subroutine

```
Procedure SOLVE(VAR trels: frame; VAR current, near, far: vec3;
VAR sol: boolean);
```

where "trels" is the $\{T\}$ frame specified relative to the $\{S\}$ frame. Other parameters are exactly as in the `INVKIN` subroutine. The definitions of $\{T\}$ and $\{S\}$ should be globally defined variables or constants. SOLVE should use calls to `TMULT`, `TINVERT`, and `INVKIN`.

3. Write a main program that accepts a goal frame specified in terms of x, y, and ϕ. This goal specification is $\{T\}$ relative to $\{S\}$, which is the way the user wants to specify goals.

The robot is using the same tool in the same working area as in Programming Exercise (Part 2), so $\{T\}$ and $\{S\}$ are defined as

$${}^{W}_{T}T = [x\ y\ \theta] = [0.1\ 0.2\ 30.0],$$

$${}^{B}_{S}T = [x\ y\ \theta] = [-0.1\ 0.3\ 0.0].$$

Calculate the joint angles for each of the following three goal frames:

$$[x_1\ y_1\ \phi_1] = [0.0\ 0.0\ -90.0],$$

$$[x_2\ y_2\ \phi_2] = [0.6\ -0.3\ 45.0],$$

$$[x_3\ y_3\ \phi_3] = [-0.4\ 0.3\ 120.0],$$

$$[x_4\ y_4\ \phi_4] = [0.8\ 1.4\ 30.0].$$

Assume that the robot will start with all angles equal to 0.0 and move to these three goals in sequence. The program should find the nearest solution with respect to the previous goal point. You should call `SOLVE` and `WHERE` back-to-back to make sure they are truly inverse functions.

MATLAB EXERCISE 4

This exercise focuses on the inverse-pose kinematics solution for the planar 3-DOF, 3R robot. (See Figures 3.6 and 3.7; the DH parameters are given in Figure 3.8.) The following fixed-length parameters are given: $L_1 = 4$, $L_2 = 3$, and $L_3 = 2$(m).

a) Analytically derive, by hand, the inverse-pose solution for this robot: Given ${}^{0}_{H}T$, calculate all possible multiple solutions for $\{\theta_1\ \theta_2\ \theta_3\}$. (Three methods are presented in the text—choose one of these.) Hint: To simplify the equations, first calculate ${}^{0}_{3}T$ from ${}^{0}_{H}T$ and L_3.

b) Develop a MATLAB program to solve this planar 3R robot inverse-pose kinematics problem completely (i.e., to give all multiple solutions). Test your program, using the following input cases:

i) $${}^{0}_{H}T = \begin{bmatrix} 1 & 0 & 0 & 9 \\ 0 & 1 & 0 & 0 \\ 0 & 0 & 1 & 0 \\ 0 & 0 & 0 & 1 \end{bmatrix}.$$

ii) $${}^{0}_{H}T = \begin{bmatrix} 0.5 & -0.866 & 0 & 7.5373 \\ 0.866 & 0.6 & 0 & 3.9266 \\ 0 & 0 & 1 & 0 \\ 0 & 0 & 0 & 1 \end{bmatrix}.$$

iii) $${}^{0}_{H}T = \begin{bmatrix} 0 & 1 & 0 & -3 \\ -1 & 0 & 0 & 2 \\ 0 & 0 & 1 & 0 \\ 0 & 0 & 0 & 1 \end{bmatrix}.$$

iv) $${}^{0}_{H}T = \begin{bmatrix} 0.866 & 0.5 & 0 & -3.1245 \\ -0.5 & 0.866 & 0 & 9.1674 \\ 0 & 0 & 1 & 0 \\ 0 & 0 & 0 & 1 \end{bmatrix}.$$

For all cases, employ a circular check to validate your results: Plug each resulting set of joint angles (for each of the multiple solutions) back into the forward-pose kinematics MATLAB program to demonstrate that you get the originally commanded ${}^{0}_{H}T$.

c) Check all results by means of the Corke MATLAB Robotics Toolbox. Try function *ikine()*.